ARTIFICIAL SATELLITES, Vol. 53, No. 4 – 2018
DOI: 10.2478/arsa-2018-0011

ENHANCED LOCAL IONOSPHERE MODEL FOR MULTI-CONSTELLATIONS SINGLE FREQUENCY PRECISE POINT POSITIONING APPLICATIONS: EGYPTIAN CASE STUDY

Emad El Manaily [1], Mahmoud Abd Rabbou [2], Adel El-Shazly [3] and Moustafa Baraka [4]
Ph.D. Candidate in Geomatic Engineering - Cairo University [1]
Assistant Prof. of Surveying and Geodesy, Faculty of Engineering - Cairo University [2]
Prof. of Surveying and Geodesy, Faculty of Engineering - Cairo University [3]
Prof. of Surveying and Geodesy, the German University in Cairo (GUC) [4]

ABSTRACT:

The positioning accuracy of single frequency precise point positioning (SFPPP) attributes mainly to the ionosphere error, which strongly affects GNSS signals. When GNSS signals pass through the various ionosphere layers, they will be bent and their speed will be changed due to dispersive nature of ionosphere. To correct the ionosphere error, it is common to use Klobuchar ionosphere model or Global Ionosphere Maps (GIM). However, Klobuchar can deal with only about 50% of the Ionosphere effect and global Ionosphere maps are often inadequate to describe detailed features of local ionosphere because of limited precision and resolution.

In this paper, an enhanced local ionosphere model was developed relying on modeling of measurements from a dense Egyptian permanent tracking GNSS network in order to achieve high precision ionosphere delay correction. The performance of the developed enhanced Egyptian ionosphere model (EIM) was verified through multi-constellations SFPPP accuracy for static and kinematic modes.

For static mode, 24 hours multi-constellations datasets collected at three selected stations, Alexandria, Cairo, and Aswan, in Egypt on February 27, 2017, to investigate the performance of the developed local ionospheric model in comparison with the Klobuchar, GIM and ionosphere free models. After session time of half an hour, the results show that the performance of static SFPPP based on the developed Egyptian ionospheric map (EIM) achieved a comparable accuracy WRT using ionosphere free model. While using EIM, achieved an improvements of (38%, 28%, and 42%) and (32%, 10%, and 37%) for accuracy of latitude, longitude, and altitude in comparison with using Klobuchar and GIM models, respectively

For kinematic mode, datasets of 2 hours of observations with 1 second sampling rate were logged during vehicular test; the test was carried out on the ring road of the city of Cairo, Egypt, on September 16, 2017. After half an hour of kinematic SFPPP data-processing, the performance of using Egyptian ionospheric map (EIM) for ionosphere delay correction, achieved an improvements of three dimension coordinates of (83%, 47%, and 62%) and (57%, 65%, and 21%) with respect to using Klobuchar model and GIM model, respectively.

Key Words: GNSS, Local Ionosphere modeling, GIM, IGS

1. INTRODUCTION

It is well known that dual-frequency, geodetic-quality GPS receivers are often used both in static and kinematic applications for high-accuracy point positioning. Dual-frequency receiver can deal with ionosphere delay error using the so called ionosphere-free linear combination of both GNSS frequencies (L1 and L2) (Seeber, G., 2003). However, using single-frequency GPS receivers in similar applications creates a challenge because of difficulty of handling the ionosphere, and other measurement error sources.

Meanwhile, the majority of mass-market GNSS users are operating single-frequency receivers due to the low costs. Consequently, the single-frequency PPP technique has received much attention from GNSS community to develop a cheap alternative to differential positioning technique, to provide comparable positioning accuracy and to significantly expand the usability of this technique in a myriad of applications where the size and cost of the GPS unit is an issue (see e.g. Øvstedal, 2002; Héroux et al., 2004; Chen and Gao 2005; Le and Tiberius 2006; Simsky 2006 Gao et al., 2006; Beran 2008; Bock et al., 2009; van Bree and Tiberius, 2011; Odijk et al., 2012).

The greatest challenge for single-frequency PPP is the treatment of ionospheric delay error which can reach tens of meters at zenith (Klobuchar 1996). The ionosphere is a shell of electrons and electrically charged atoms and molecules that surrounds the Earth, stretching from a height of about 50 km to more than 1,000 km. It exists primarily due to ultraviolet radiation from the Sun (Hargreaves, 1992). Moreover, the ionosphere is highly unpredictable and its condition depends mainly on geographic location, time of the day, season of the year, and solar activity. The free electrons in ionosphere layer exert severe perturbations on the propagation of microwave signals transmitted continuously by GNSS satellites. These Perturbations may occur to the direction of propagation, to the velocity of propagation and to the signal strength. Moreover, the ionosphere is a dispersive medium, and that therefore the phase velocity (propagation of the carrier) is not the same as the group velocity (propagation of the codes). Consequently, ionosphere influences have to be determined directly by measurements and/or by modeling, and they have to be considered within the adjustment process (Seeber, G., (2003).

Actually, several methods are used to eliminate the ionosphere errors. For example, GNSS satellites broadcast the parameters of the Klobuchar ionosphere model for single frequency users. The Klobuchar model was designed to minimize user computational complexity and user computer storage as far as to keep a minimum number of coefficients to transmit on satellite-user link. These parameters model the effect of the ionosphere on the GNSS signal but can account only for about 50% of the total effect (Klobuchar 1987).

In 1998, IGS has started a working group to develop global ionospheric gridded data representing the total electron content over the whole globe. The vertical TEC values (VTEC) and DCBs, in the IONospheric Exchange (IONEX) format (Schaer et al., 1998), are obtained from seven analysis centers (IAACs) (Roma, David et al., 2017). The ionospheric delay is corrected using the daily combined IGS Final GIM, which is accurate to 2 −8 TECU (1 TECU corresponds to a delay of 0.16 m on L1 frequency) (Hernández-Pajares et al. 2009). For more information about the GIM, refer to the IGS website (http://www.igs.org). However, global TEC maps have limited precision and resolution in some areas like North of Africa that there are no IGS stations in Egypt which in role affected the accuracy of using IGS GIM product in Egypt, as shown in figure 1.

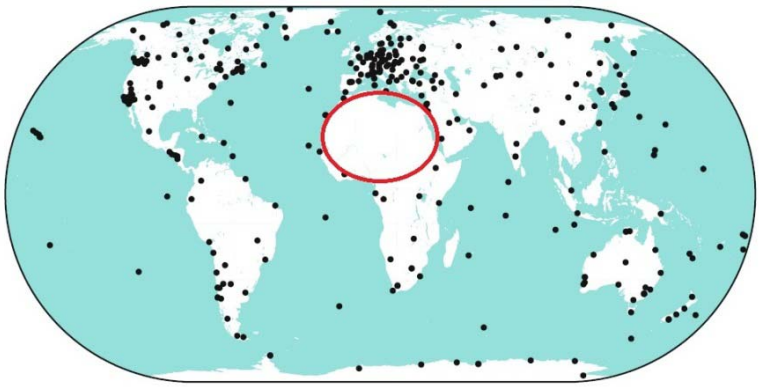

Figure 1. Global distribution of IGS stations

To deal with the holes of the first GIM computation stage existing in the North Africa and over the Oceans resulting from a shortage of GNSS stations in North Africa, an optimum spatial-temporal interpolation technique was developed to cover these holes (Krankowski and Hernandez-Pajares, 2016). Moreover, due to the lack of GPS stations over the equatorial, North Africa and Atlantic ocean in IGS network, the produced Global Ionospheric maps (GIMs) have poor effect for mitigating ionospheric error for precise positioning (Mostafa RABAH et al, 2018).

Consequently, local ionosphere model is required to provide high precision ionosphere delay correction. The obtained local ionosphere model typically relies on modeling of measurements from the permanent tracking stations which known as Egyptian virtual reference stations (VRS), in order to achieve high precision. The proposed ionosphere maps are generated on a daily basis using data from about 40 GNSS stations along Nile valley and its Delta. The Targeting temporal resolution is two-hours and spatial resolution of 0.5° and 0.5° in longitude and latitude, respectively. The derived Egyptian ionosphere maps (EIMs), was validated as mitigation of the ionospheric errors in comparison with Klobuchar model and the Global Ionospheric Maps (GIMs). Also, we tried to evaluate the performance of SFPPP supported by EIM for different applications.

2. MATHEMATICAL SINGLE FREQUENCY GNSS PPP MODEL

Considering the multi-GNSS observations including GPS, GLONASS, Galileo and BeiDou, the mathematical model for single frequency GNSS PPP can be written as (Abd Rabbou and El-Rabbany, 2015):

$$\boldsymbol{P_G = \varrho_G + c(dt - b_G^r) - c\,d\overline{T_G} + d_G^{ion} + d_G^{trop} - c(B_G^s) + \varepsilon_G} \quad (1)$$

$$\boldsymbol{P_j = \varrho_j + c(dt - b_G^r) - c\,d\overline{T_J} + d_j^{ion} + d_j^{trop} - c(B_j^s) + c[ISB_j] + \varepsilon_G} \quad (2)$$

$$\boldsymbol{\Phi_G = \varrho_G + c(dt - b_G^r) - c\,d\overline{T_G} - d_G^{ion} + d_G^{trop} - c(B_G^s) + [\lambda\overline{N_G} + c\,(\delta_G - d_G) - c\,(\delta_G^S - d_G^S)] + \varepsilon_G} \quad (3)$$

$$\boldsymbol{\Phi_j = \varrho_j + c(dt - b_G^r) - c\,d\overline{T_J} - d_j^{ion} + d_j^{trop} - c(B_j^s) + c[ISB_j] + [\lambda\overline{N_J} + c\,(\delta_j - d_j) - c\,(\delta_j^S - d_j^S)] + \varepsilon_j} \quad (4)$$

Where G is GPS system, j is other global navigation system (GLONASS, Galileo and Beidou); $d\overline{T_G}$ and $d\overline{T_J}$ are satellites clock error, for GPS and the other global navigation systems respectively, lumped with the ionosphere-free differential code bias, which can be obtained from the IGS-MGEX (Montenbruck et. al., 2014); d_1^{ion} is the ionospheric delay component in meters; d_1^{trop} is the tropospheric delay component in meters; B_G^s and B_j^s are a bias terms, for GPS and the other global navigation systems respectively, representing the combined effect of differential code bias of the satellite, as shown in Table 1: ISB is the inter-

system biases; ε_G and ε_j are relevant system noise and un-modeled residual errors for GPS the other navigation systems respectively.

Table 1. GNSS single frequency observations processed and differential code biases corrections applied.

GNSS system	Observations used in SF Processing	Observations processed in satellite clock estimation	Bias term B
GPS	C1C (C/A) and L1C	C1P and C2P	$DCB_{P1C1}+\frac{f_2^2}{f_1^2-f_2^2}DCB_{P1P2}$
GLONASS	C1P and L1P	C1P and C2P	$\frac{f_2^2}{f_1^2-f_2^2}DCB_{P1P2}$
Galileo	C1X and L1X (E1)	C1X and C5X	$\frac{f_5^2}{f_1^2-f_5^2}DCB_{C1XC5X}$
BeiDou	C2I and L2I	C2I and C7I	$\frac{f_7^2}{f_2^2-f_7^2}DCB_{C2IC7I}$

In our single-frequency GNSS model, the GPS receiver hardware delay b_G^r is lumped to the receiver clock error and the combined receiver clock bias is considered as a single unknown in our estimation filter. As a result, the ISB for each GNSS system is given by:

$$ISB_j = [d_G - d_j] + GJ_{T.off} \tag{5}$$

Where $GJ_{T.off}$, is the GPS/other global navigation system (GLONASS, Galileo and Beidou) system time offsets, respectively, which result from the differences in the system time scales. These time offsets will exist if the broadcast ephemeris of each system is used. However, since the precise satellite clock corrections from MGEX are used, which are referred to the GPS time, the time offsets will disappear in Equations (5) (Fei Guo et. al., 2016).

The differential code biases DCBs can be obtained from the IGS MGEX archive (Wang et al 2016; Montenbruck et. al., 2014). The UNB3 tropospheric model, consisting of the Saastamoinen vertical propagation delay model and Niell mapping function, is used to account for the dry component of the tropospheric delay (Leandro et al. 2008). The existing models are used to account for the effects of ocean loading, Earth tide, carrier-phase windup, sagnac, relativity, and satellite antenna phase-center variations (Kouba 2009). Considering the above corrections, the final mathematical model for single frequency GNSS PPP can be simplified to:

$$\overline{P_G} = \sqrt{(x_r - X_G^s)^2 + (y_r - Y_G^s)^2 + (z_r - Z_G^s)^2} + d_G^{ion} + m_w zwd + c\,d\bar{t_r} + \dot{e_G} \tag{6}$$

$$\overline{P_J} = \sqrt{(x_r - X_j^s)^2 + (y_r - Y_j^s)^2 + (z_r - Z_j^s)^2} + d_j^{ion} + m_w zwd + cd\bar{t_r} + c[ISB_j] + \dot{e}_j \tag{7}$$

$$\overline{\Phi_G} = \sqrt{(x_r - X_G^s)^2 + (y_r - Y_G^s)^2 + (z_r - Z_G^s)^2} - d_G^{ion} + m_w zwd + c\,d\bar{t_r} + A_G + \dot{\varepsilon_G} \tag{8}$$

$$\overline{\Phi_J} = \sqrt{(x_r - X_j^s)^2 + (y_r - Y_j^s)^2 + (z_r - Z_j^s)^2} - d_j^{ion} + m_w zwd + c\,d\bar{t_r} + A_j + c[ISB_j] + \dot{\varepsilon}_j \tag{9}$$

where $\overline{\mathrm{P}}$ and $\overline{\Phi}$ are the corrected pseudorange and carrier phase measurements, respectively; G is GPS system, j is other global navigation system (GLONASS, Galileo and Beidou); x_r, y_r and z_r are the unknown receiver coordinates; X^s, Y^s and Z^s are the satellite coordinates obtained from the final IGS-MGEX orbital products and corrected for the effect of earth rotation during signal transit; As indicated above, local ionospheric model (EIM) is used to account for the ionospheric delay (d_G^{ion} and d_j^{ion}), in comparison of effect of other models. The wet troposphere delay ($m_w zwd$) is less predictable and, thus, it is considered as unknown parameter by the standard SFPPP algorithm in the estimation process as (m_w) is the wet mapping factor and (zwd) is the wet component of the tropospheric delay; $\bar{\mathrm{d}}\mathrm{t_r}$ is receiver

clock error lumped with the GPS receiver hardware delay as stated in Equations (6) to (9); ê and ε̂ are are relevant system noise and un-modeled residual errors dumped by additional ionospheric residuals; A is the ambiguity term.

3. METHODOLOGY OF DRIVING LOCAL IONOSPHERE MODEL

A single-layer model which is based on the corresponding mapping function is used to model the ionospheric Total Electron Content (TEC) using the geocentric latitude and the sun-fixed longitude of the ionosphere pierce point (IPP). These model has the advantage over Taylor series expansions, to be well suited for regional and for global models (Schaer, 1995).

The slant total electron content (*STEC*) is estimated from GNSS dual-frequency observations considering smoothed pseudo-range based geometry-free $\boldsymbol{P_{4s}}$ as follow

$$\boldsymbol{P_{4s}} = \mathbf{40.3} * \mathbf{10^{16}}\left(\frac{1}{f_2^2} - \frac{1}{f_2^2}\right) \boldsymbol{STEC} + \boldsymbol{DCB_r} - \boldsymbol{DCB^s} \quad (10)$$

$$\boldsymbol{STEC} = -\frac{f_1^2 f_2^2}{\mathbf{40.3} * \mathbf{10^{16}}\left(f_1^2 - f_2^2\right)} \left(\boldsymbol{P_{4s}} - \boldsymbol{DCB_r} + \boldsymbol{DCB^s}\right) \quad (11)$$

Where ($\boldsymbol{DCB_r}$, & $\boldsymbol{DCB^s}$) are differential code bias for receiver and satellites, respectively. Commonly, the ionosphere is assumed to be concentrated in a thin layer at altitude *H*, as a result, the *STEC* can be translated into the vertical total electron content (*VTEC*) using the modified single-layer model (*MSLM*) as used in CODE *VTEC* products by defining a mapping function (*MF*)

$$\mathbf{MF}\,(\mathbf{v}) = \mathbf{cos}[\mathbf{arcsin}\,(\frac{\mathbf{R}}{\mathbf{R+H}}\,\mathbf{sin}\,(\boldsymbol{\alpha}\mathbf{v}))] \quad (12)$$

$$\boldsymbol{VTEC} = \boldsymbol{MF}\,(\boldsymbol{v})\,\boldsymbol{STEC} \quad (13)$$

Where $\boldsymbol{v}$ is the satellite elevation angle, *R* is the earth's radius, and *H* is the attitude of the ionosphere thin layer (normally the approximate peak height of the *F2* layer). *R* is set to 6,371 km. *H* and α can be set by users. Commonly, they are defaulted as *H* = 506.7 km and *a* = 0.9782, which are consistent with the values used by the CODE group. Adjusted spherical harmonic function, with just degree and order of (5), are used in establishing the national ionospheric model. These spherical harmonic function are applied to simulate the *VTEC* as *E(φ, η)* which can be expressed as follows (Schaer 1999):

$$\boldsymbol{VTEC} = \boldsymbol{E}\,(\boldsymbol{\varphi}, \boldsymbol{\eta}) = \sum_{n=0}^{n_{max}} \sum_{m=0}^{m} \boldsymbol{P_{mn}}\,(\mathbf{sin}\,\boldsymbol{\varphi})\,(\boldsymbol{a_{nm}}\,\mathbf{cos}\,\boldsymbol{m\eta} + \boldsymbol{b_{mn}}\,\mathbf{sin}\,\boldsymbol{m\eta}) \quad (14)$$

Where $\boldsymbol{\varphi}$ is the geocentric latitude of the ionosphere pierce point (IPP), η = λ - λ0 is the sun-fixed longitude of the IPP: λ and λ0 are the longitude of the IPP and the apparent solar time, respectively, a_{mn} and b_{mn} are the regional ionosphere model coefficients, P_{mn} are normalized Legendre polynomials. Substituting Equation (11) and (12) into Equation (13), the following expression can be obtained:

$$\boldsymbol{VTEC} = \sum_{n=0}^{n_{max}} \sum_{m=0}^{n} \boldsymbol{P_{mn}}\,(\mathbf{sin}\,\boldsymbol{\varphi})\,(\boldsymbol{a_{nm}}\,\mathbf{cos}\,\boldsymbol{m\eta} + \boldsymbol{b_{mn}}\,\mathbf{sin}\,\boldsymbol{m\eta})$$

$$= \mathbf{cos}\left[\boldsymbol{arcsin}\left(\frac{\boldsymbol{R}}{\boldsymbol{R+H}}\,\boldsymbol{sin}\,(\boldsymbol{\alpha v})\right)\right]\left[-\frac{f_1^2 f_2^2}{\mathbf{40.3} * \mathbf{10^{16}}\,(f_1^2 - f_2^2)}\,(\boldsymbol{P_{4s}} - \boldsymbol{DCB_r} + \boldsymbol{DCB^s})\right. \quad (15)$$

where a_{mn} , b_{mn} , DCB_r and DCB^S are the estimated unknown parameters. The area of study defines the order of spherical harmonics expansion. Commonly, for Egyptian region, 5th order is sufficient. The set of the ionosphere coefficients will be assumed every 2 h to be consistent with GIM model, for one GPS station; there are more than 20,000 measurements every day (epoch time 30 sec). Thus, the number of observations is much more than the number of unknown parameters. According to the theory described above, the DCB and ionosphere coefficients can be estimated from GPS dual frequency observations by the least squares (LS) method. However, due to the singularity of Equation (15), additional constrain should be added to separate the satellite and receiver differential code biases. Traditionally,

the sum of all GNSS satellite DCB values is assumed to be zero. Under this constraint condition, Equation (15) reaches full rank and the DCBs of the satellites and receivers can be separated.

Five years ago, Egypt established a continuous operating reference stations network (CORS) along Nile valley and its Delta to mainly overcome the problems of GPS campaign and guarantee that the surveying works all over the country to be unified in the same datum. The CORS stations cover the country from Mediterranean Sea at the North to Aswan at the South and it consists of 40 stations as shown in Figure 2.

The continuous operating reference stations network (CORS) consists of 40 stations spaced by distances that range from 50 km to 70 km. The stations are equipped with dual frequency GNSS receivers (Trimble Net R8). The GPS/GLONASS reinex observations of 35 stations are collected and processed by our developed MATLAB software.

MATLAB software called EGY_ION is developed to model the mathematical equations presented in the previous Section. The software is include five main functions: a MATLAB function reading the GNSS RINEX files to exclude the GNSS observations, a MATLAB function navigation messages to exclude the satellite coordinates in real time, a Matlab function to apply the geometry free linear combinations for pseudo-range and phase observations, a MATLAB function to apply a phase based smoothing for the pseudo-range geometry free linear combination observations, a MATLAB function for the least square estimator for Equation (15), in addition to other secondary calculation functions. Figure 3 shows the flow chart for the proposed software.

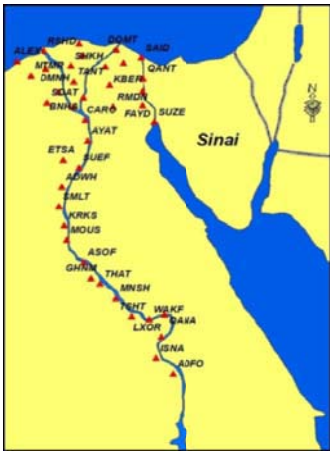

Figure 2. Egyptian GNSS continuous operating reference stations network

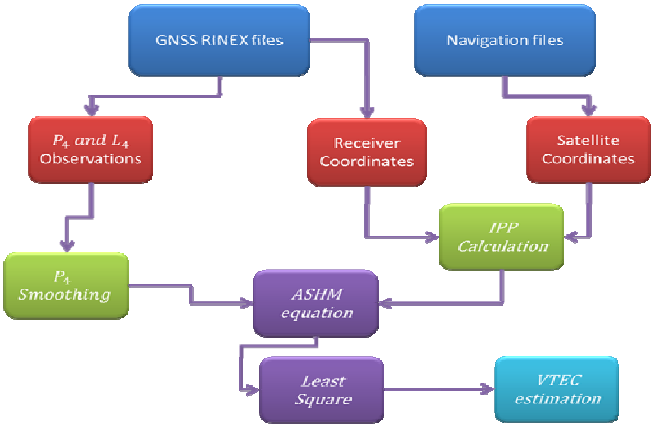

Figure 3. EGY_ION flow chart

The obtained Egyptian Ionosphere model (EIM) has temporal resolution of two-hours and spatial resolution of 0.5° and 0.5° in longitude and latitude, respectively, which is considered to be better model for ionospheric information than the products provided by GIM which is basically interpolated for this area. Figure 4 shows TEC snapshots taken at 00:00, 02:00, 04:00, 06:00..... 24:00 UTC with contour lines are given for every 0.5 TECU. As shown in the TEC snapshots, Ionosphere is highly temporal and spatial variable. Moreover, ionization increases in the sunlit hemisphere, especially at noon, where TEC values range from 35 TECU to 77.8 TECU (Red Maps) and decreases on the shadowed side at night, for example, the snapshot of 02:00 AM where TEC values range from 7.2 TECU to 9.5 TECU (Pale Yellow).

On the other hand, Figure 5 Root mean square "RMS maps snapshots" covering both the daytime and nighttime periods taken at 00:00, 02:00, 04:00, 06:00..... 24:00 UTC with contour lines are given for every 0.05 TECU.

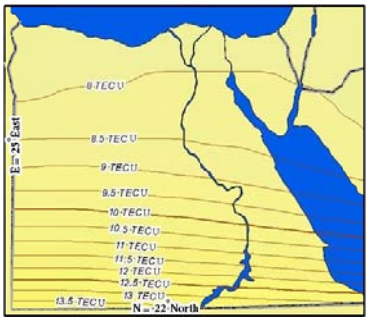

TECU map snapshot at
Feb 27, 2017, 00:00:00 UTC

TECU map snapshot
Feb 27, 2017, 02:00:00 UTC

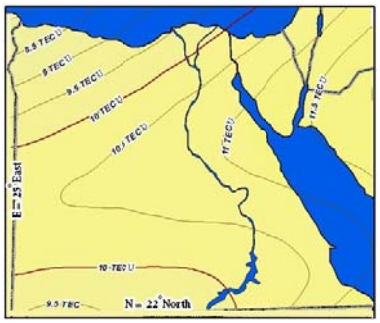

TECU map snapshot
Feb 27, 2017, 04:00:00 UTC

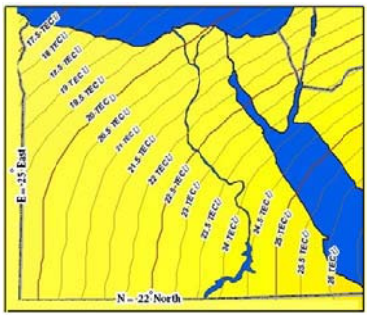

TECU map snapshot at
Feb 27, 2017, 06:00:00 UTC

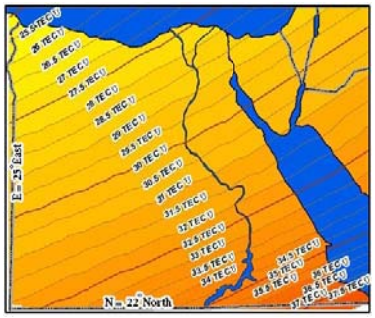

TECU map snapshot
Feb 27, 2017, 08:00:00 UTC

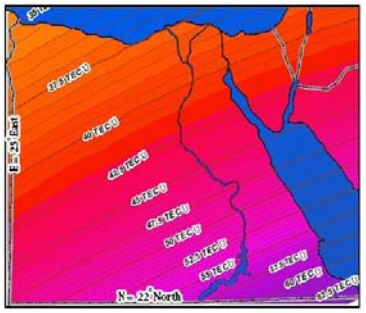

TECU map snapshot
Feb 27, 2017, 10:00:00 UTC

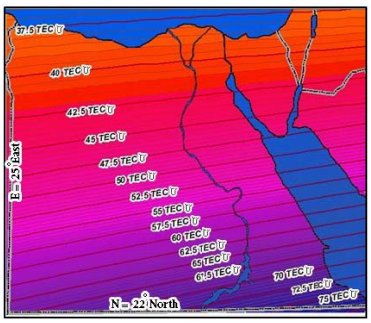

TECU map snapshot at
Feb 27, 2017, 12:00:00 UTC

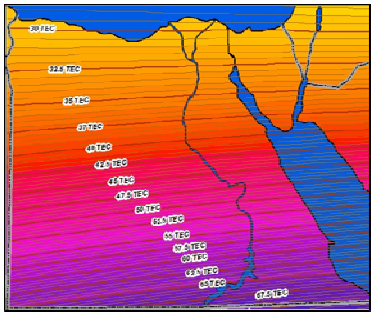

TECU map snapshot
Feb 27, 2017, 14:00:00 UTC

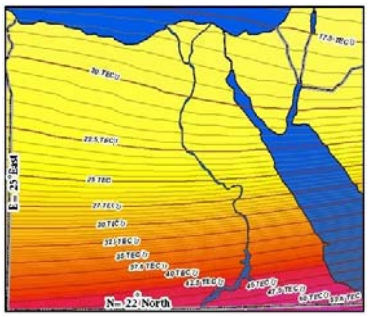

TECU map snapshot
Feb 27, 2017, 16:00:00 UTC

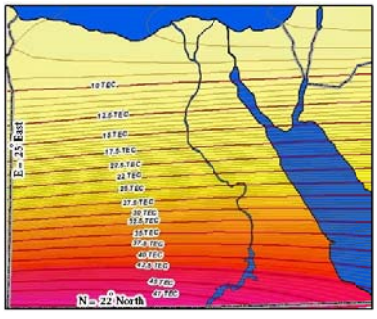

TECU map snapshot at
Feb 27, 2017, 18:00:00 UTC

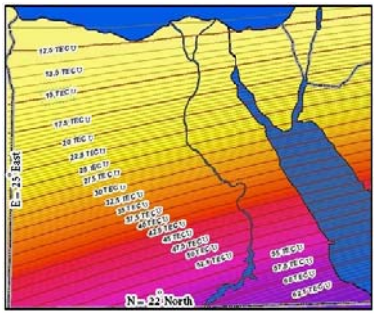

TECU map snapshot
Feb 27, 2017, 20:00:00 UTC

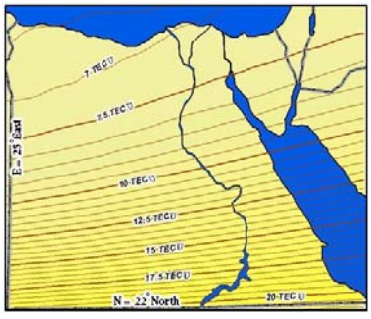

TECU map snapshot
Feb 27, 2017, 22:00:00 UTC

Figure 4. Egypt National vertical Total Electron Content

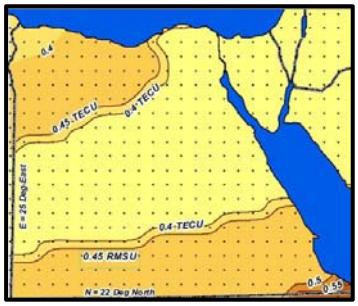

RMS map snapshot at
Feb 27, 2017, 00:00:00 UTC

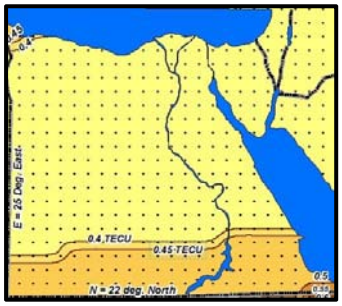

RMS map snapshot
Feb 27, 2017, 02:00:00 UTC

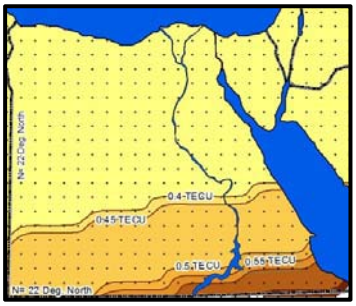

RMS map snapshot
Feb 27, 2017, 04:00:00 UTC

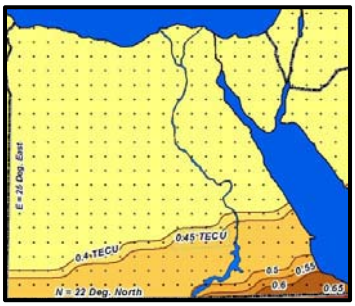

RMS map snapshot
Feb 27, 2017, 06:00:00 UTC

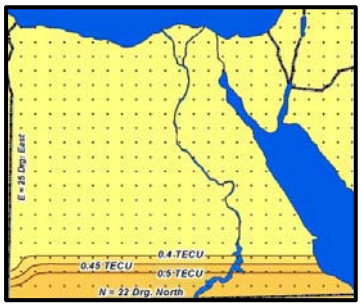

RMS map snapshot
Feb 27, 2017, 08:00:00 UTC

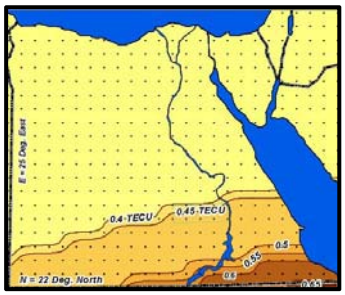

RMS map snapshot
Feb 27, 2017, 10:00:00 UTC

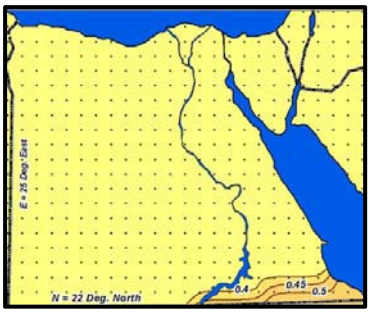

RMS map snapshot at
Feb 27, 2017, 12:00:00 UTC

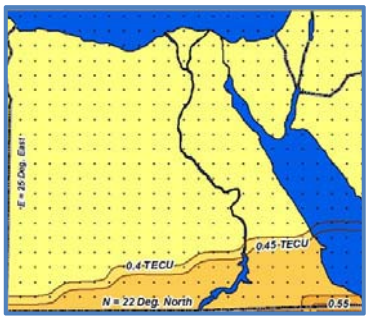

RMS map snapshot
Feb 27, 2017, 14:00:00 UTC

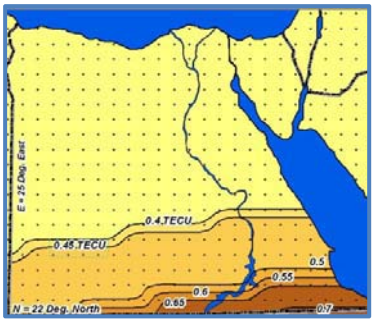

RMS map snapshot
Feb 27, 2017, 16:00:00 UTC

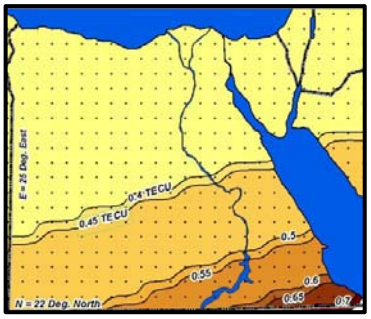

RMS map snapshot at
Feb 27, 2017, 18:00:00 UTC

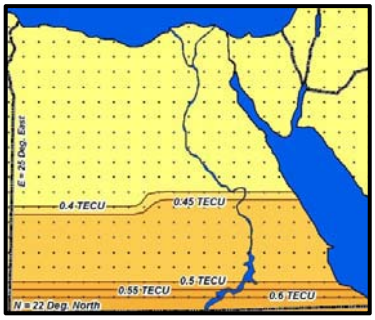

RMS map snapshot
Feb 27, 2017, 20:00:00 UTC

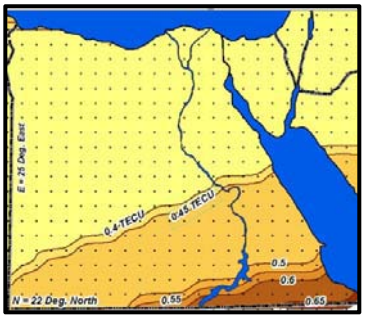

RMS map snapshot
Feb 27, 2017, 22:00:00 UTC

Figure 5. RMS maps snapshots covering both the daytime and nighttime periods

4. SINGLE FREQUENCY PPP TESTS AND RESULTS

As said before, the main target of this work is to evaluate of SFPPP supported by EIM. Consequently, the positioning accuracy of SFPPP based on EIM was examined in all applications modes, static and kinematic, in comparison with other ionosphere models. The results are shown and commented in the next sections.

4.1. Static Single Frequency PPP Tests and Results

Multi-constellations 24 hours datasets were collected at three selected stations in Egypt at different latitudes to cover the country namely: Alexandria, Cairo, and Aswan on February 27, 2017, as appeared in Figure 6, while table 2 shows the coordinates of these stations. These data sets are used to evaluate the performance of SFPPP based on the developed Egyptian ionospheric map (EIM), in static mode.

The average results show that, the performance of SFPPP based on the developed Egyptian ionospheric map (EIM) achieved a comparable accuracy WRT that of ionosphere free model and an improvements of (38%, 28%, and 42%) and (32%, 10%, and 37%) for accuracy of latitude, longitude, and altitude in comparison with SFPPP with Klobuchar model, and GIM model, respectively, after session time of half an hour of static datasets. Figure 7 shows SFPPP positioning accuracy for station of Cairo, while Figure 8 shows the RMSE for latitude, longitude and altitude of Klobuchar, GIM and EIM models for that station.

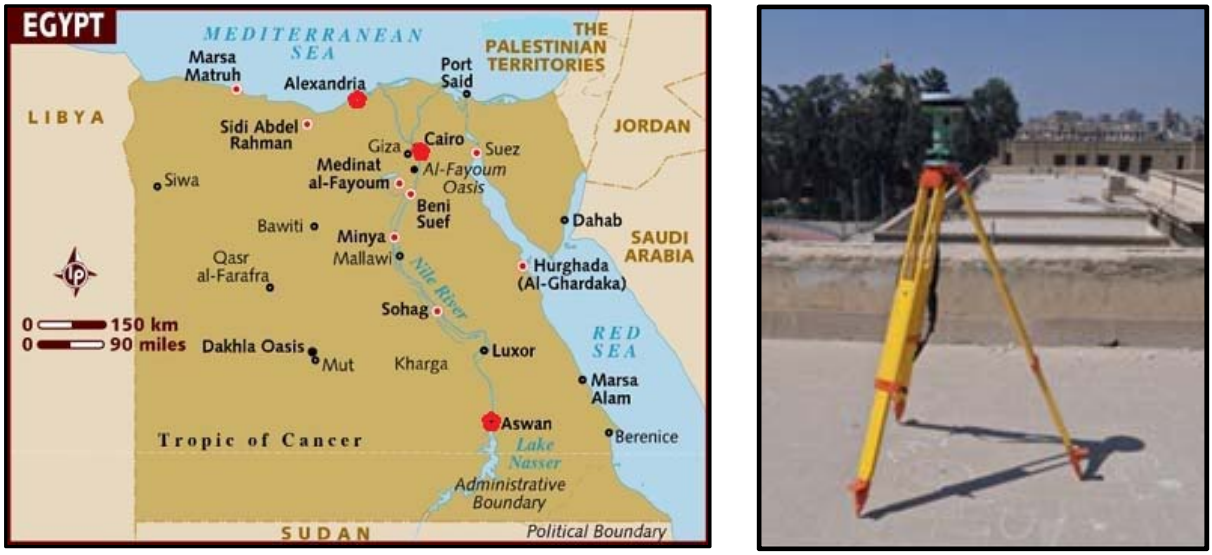

.**Figure 6.** The three selected GNSS stations.

Table 2. Coordinates of three selected stations in Egypt

Station Name	Latitude	Longitude	Up
ALEX	31 12 14.1622 N	29 54 16.9802 E	66.851 m
CARO	30 01 55.7181 N	31 12 55.0524 E	75.579 m
ASWN	24 06 25.7835 N	32 54 07.1222 E	112.658 m

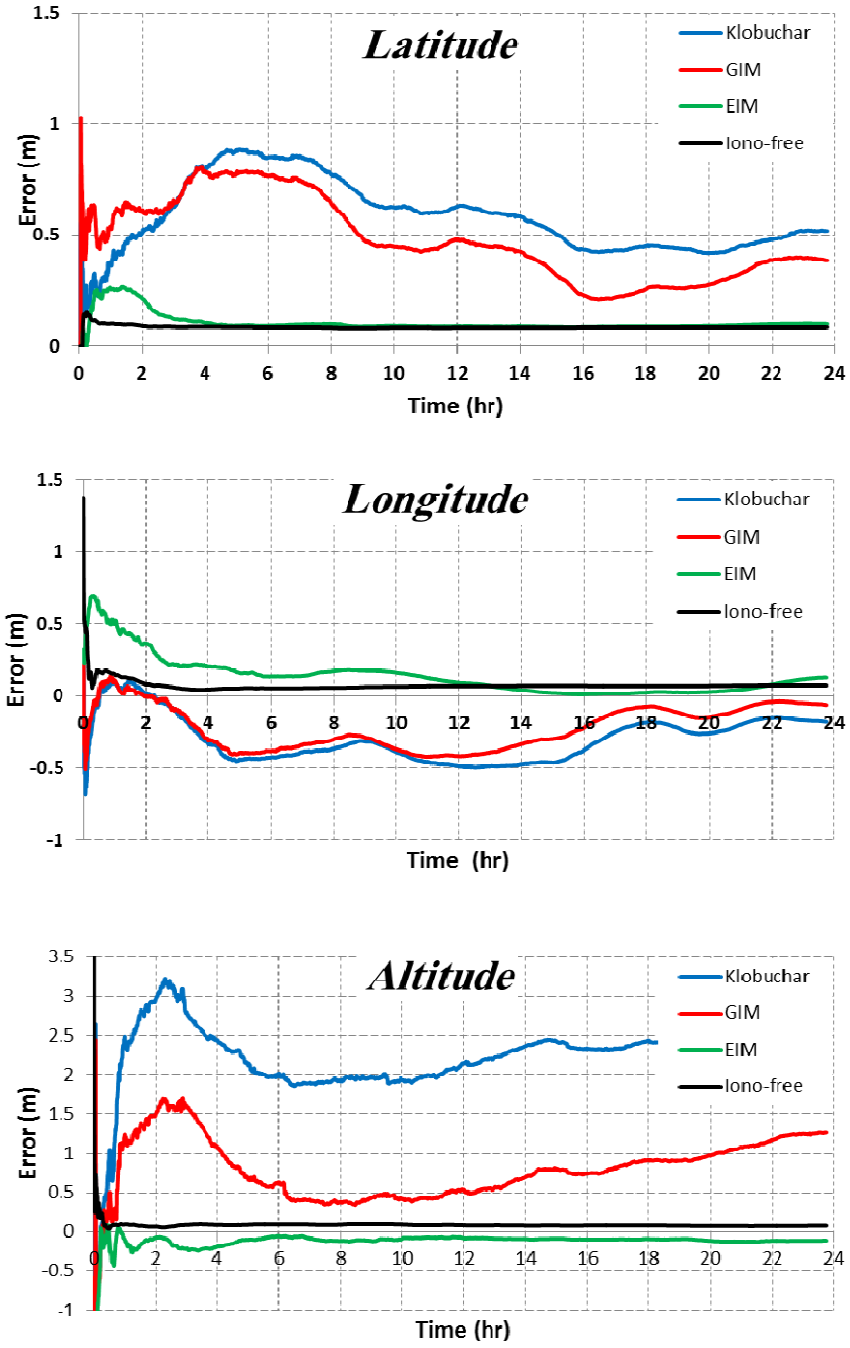

Figure 7. SFPPP Position accuracy for Station of CAIRO.

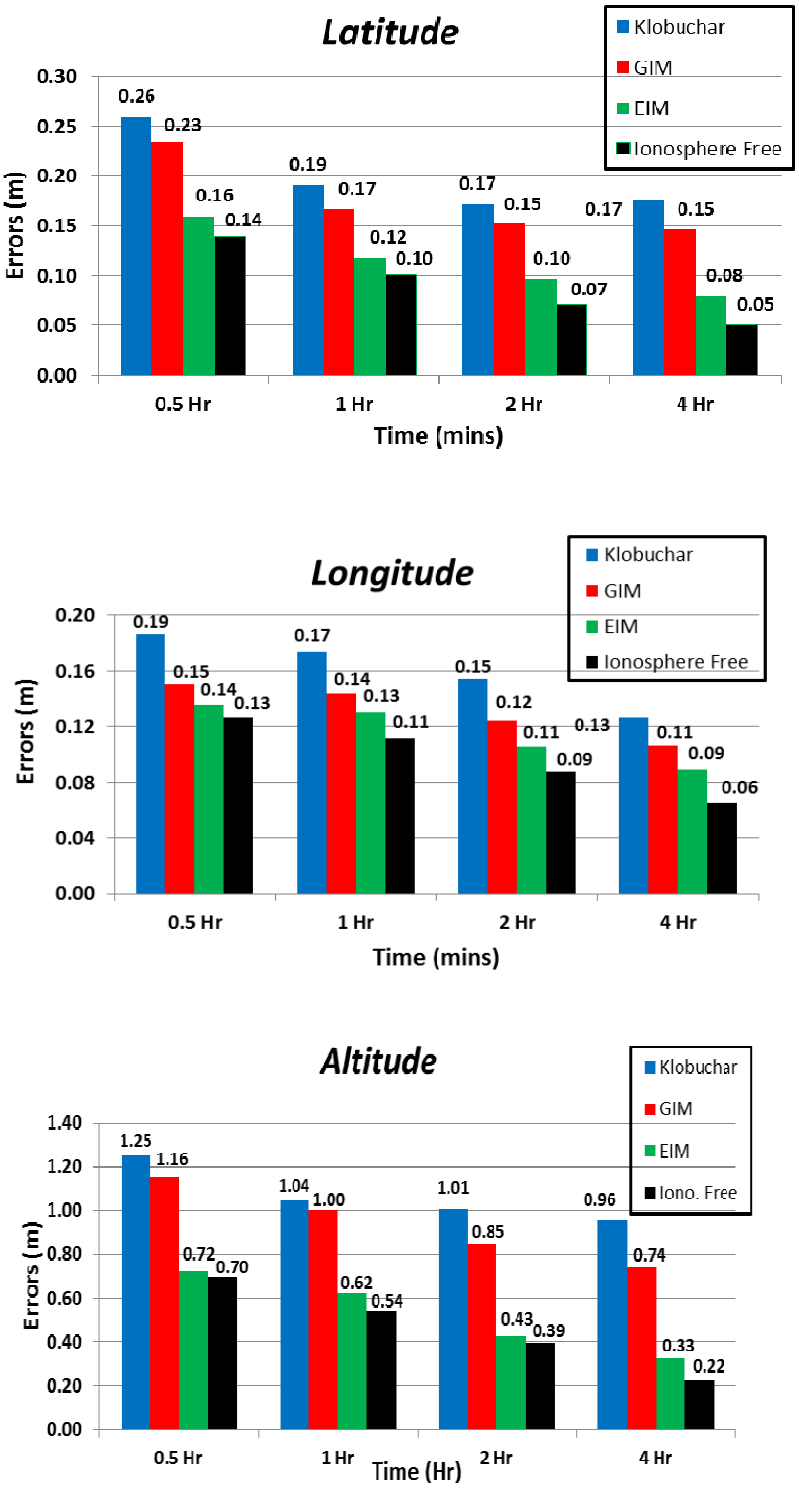

Figure 8. The RMSE for latitude, longitude and altitude for Cairo station

On the other hand, figures (9a), (9b) and (9c) show the improvement of accuracy of latitude, longitude and altitude of stations Alex, Cairo and Aswan due to using local ionosphere model with respect to klobuchar and GIM after session time of 0.5 Hr and 4.0 Hr. the results show the significant of using EIM for single frequency PPP as follow:

- For **latitude**: an improvement of accuracy due to EIM varied from 29% to 63% WRT using of klobuchar and from 17% to 50% WRT using of GIM.
- For **longitude**: an improvement of accuracy due to using EIM varied from 17% to 45% WRT using of klobuchar and from 10% to 52% WRT using of GIM.
- For **altitude**: an improvement of accuracy due to using EIM varied from 17% to 45% WRT using klobuchar and from 10% to 52% WRT using GIM.

As said before ionosphere is highly unpredictable, moreover, Klobuchar can deal with only about 50% of the Ionosphere effect and global Ionosphere maps are often inadequate to describe detailed features of local ionosphere because of the lack of GNSS stations over North Africa in IGS network, the produced Global Ionospheric maps (GIMs) have less effect for mitigating ionospheric error. Consequently, the results show that local ionosphere model provide high precision ionosphere delay correction.

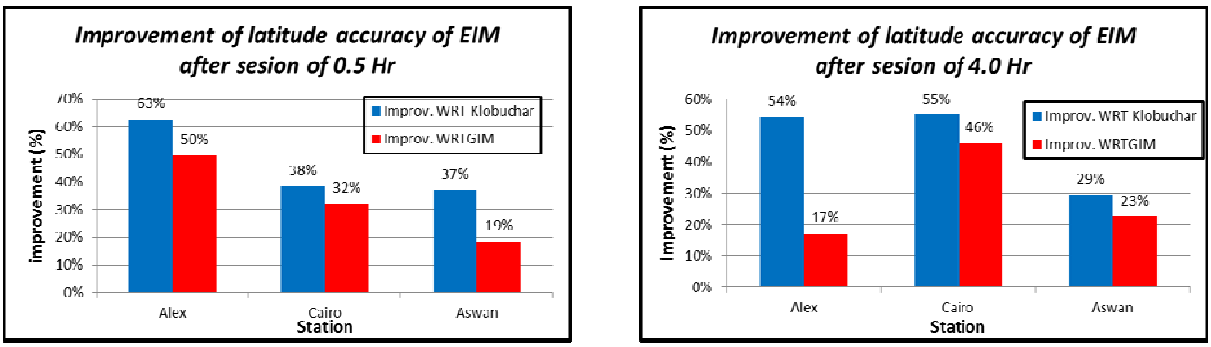

Figure 9a. Improvement of latitude accuracy of "EIM" WRT "klobuchar" and "GIM".

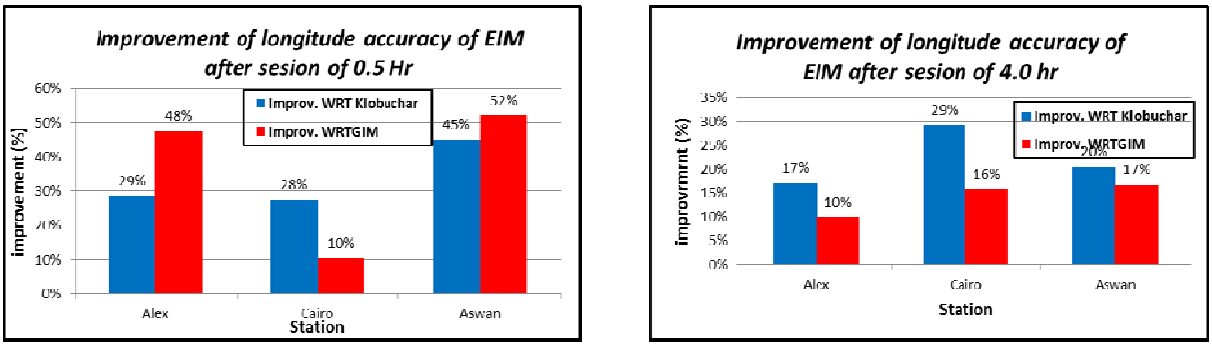

Figure 9b Improvement of longitude accuracy of "EIM" WRT "klobuchar" and "GIM".

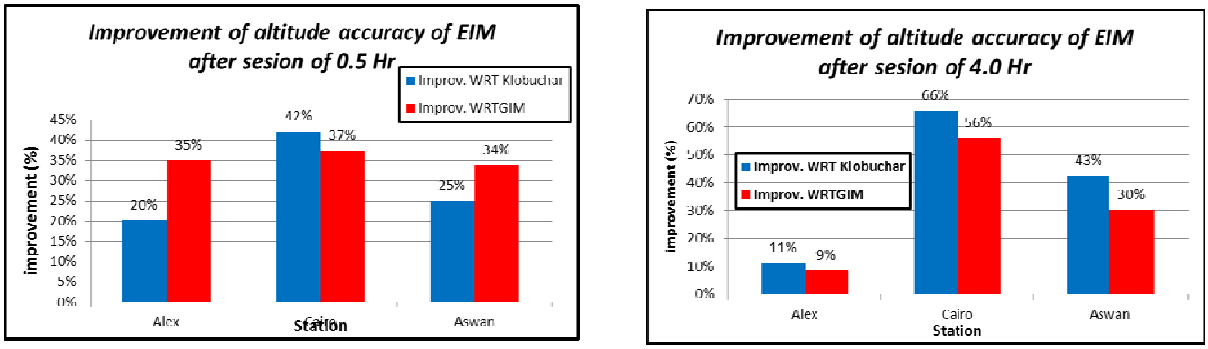

Figure 9c. Improvement of longitude accuracy of "EIM" WRT "klobuchar" and "GIM".

4.2. Kinematic Single Frequency GNSS PPP Tests and Results

A vehicular test was conducted in order to evaluate the performance of multi-constellation kinematic SFPPP based on using (EIM) model. The test was carried out on the ring road of the City of Cairo, Egypt, on September 16, 2017. Leica GS15 GNSS receiver was employed to collect the kinematic multi-constellation GNSS observations, as shown in Figure 10. The positioning accuracy was assessed in comparison with differential GNSS (DGNSS) solution by setting up a reference solution, Leica GS15 receiver, on one of the buildings of Faculty of Engineering Cairo University as a nearby base station with precisely known coordinates.

Figure 10. Vehicular test

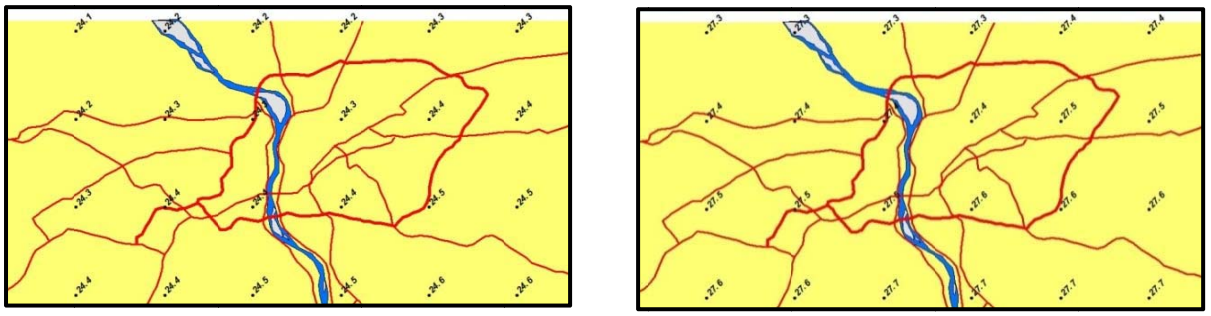

Figure 11. TEC values of local ionosphere map of great Cairo at 10 AM and 12 AM

Moreover, to evaluate kinematic SFPPP based on using (EIM) model, a local ionosphere model was derived by collecting 24 hours datasets of 25 Egyptian CORS stations, with 30 second sampling rate, on the same day (September 16, 2017) and processed by the developed MATLAB software EGY_ION to produce local ionosphere map of area of great Cairo. The obtained local ionosphere model (EIM) had temporal resolution of two-hours and spatial resolution of 0.1° in latitude and 0.1° in longitude. Figures 11 show snapshots of TEC values of local ionosphere map of great Cairo at 10 AM and at noon (12 AM).

On the other hand**,** Figure 12 shows the SFPPP positioning accuracy of latitude, longitude and altitude for kinematic observations of ring road of Cairo using different mitigation methods of ionosphere delay errors; the proposed EIM models, Klobuchar, GIM, and ionosphere free model. While Figure 13 shows corresponding root mean square of SFPPP positioning accuracy. Overall, it can be seen that the accuracy of ionosphere free model was far higher than the other models, since it cancel out the effect of ionosphere. However, this model cannot be used for single frequency receiver.

Considering the other three models which used for single frequency observations, the accuracy of latitude, longitude and altitude were significantly lower. However, using local ionosphere model (EIM) achieved the highest accuracy amongst them.

For latitude, EIM based SFPPP, with RMSE of "0.30 m to 0.48 m" at sessions of "0.5 Hr to 2 Hr", showed an improvements of accuracy of (83 % to 81%) and (57% to 64%) in comparison with that used klobuchar and GIM models, respectively.

For longitude, EIM based SFPPP, with RMSE of "1.04 m to 1.02 m" at sessions of "0.5 Hr to 4 Hr", showed an improvements of accuracy of (47 % to 70%) and (-65% to 32%) in comparison with that used klobuchar and GIM models, respectively.

For Altitude, EIM based SFPPP, with RMSE of "1.04 m to 1.17 m" at sessions of "0.5 Hr to 4 Hr", show improvements of accuracy of (62 % to 67%) and (21% to 54%) in comparison with that used klobuchar and GIM models, respectively.

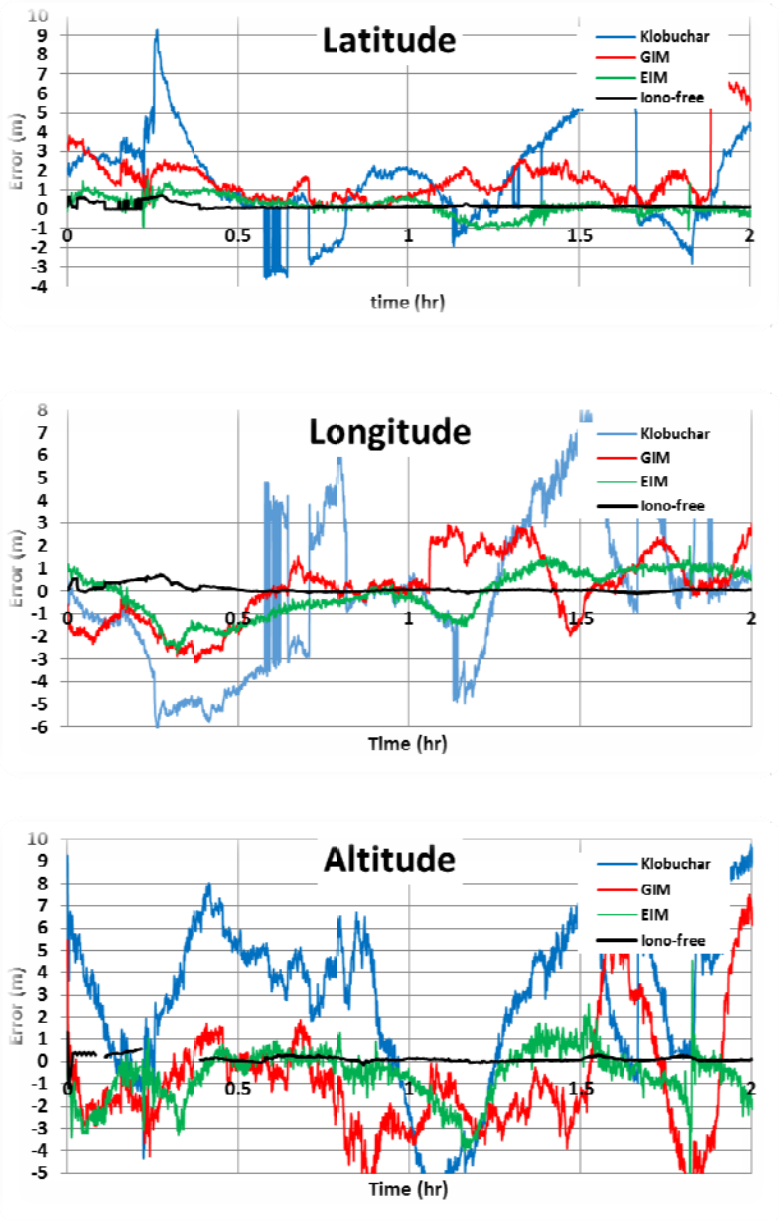

Figure 12. SFPPP Position accuracy

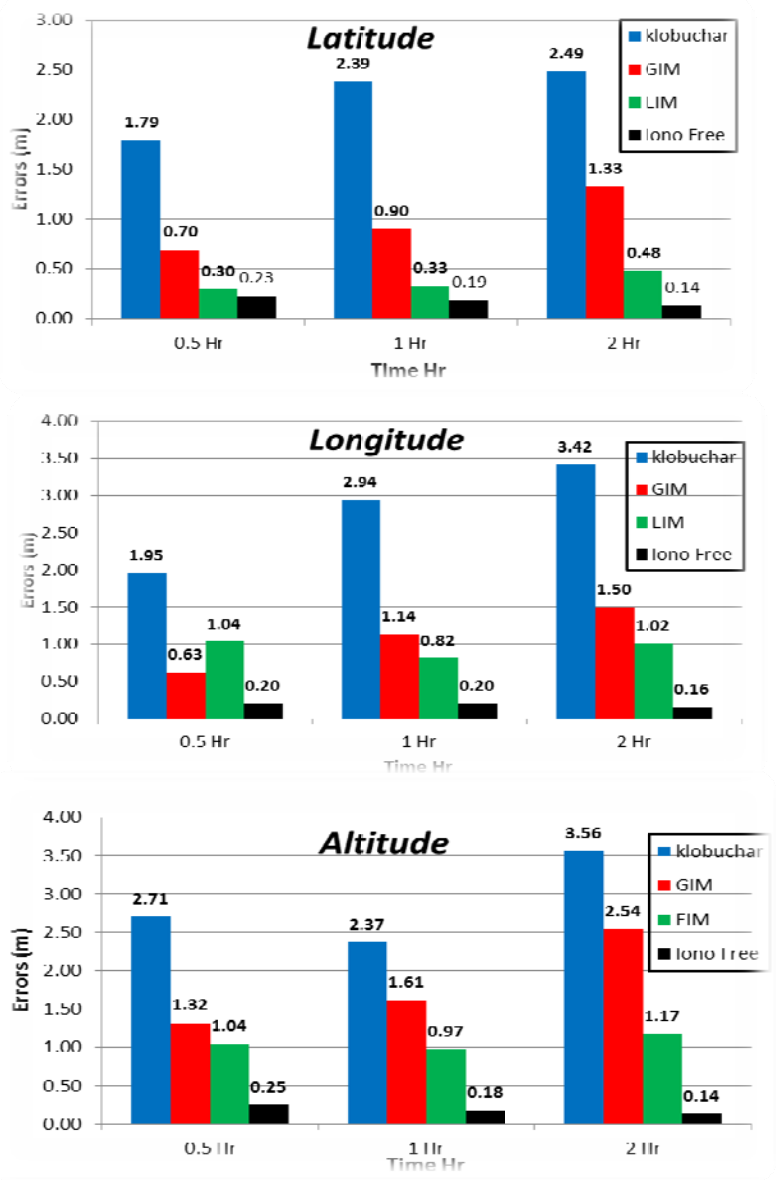

Figure 13. The RMSE for latitude, for kinematic observation of Cairo ring road longitude and altitude of Cairo ring road

5. CONCLUSION

In this paper, Egyptian ionospheric maps (EIM), was developed based on national GNSS network. The slant TEC values along the GNSS signal paths were quantified using smoothed pseudo-range based geometry-free $\boldsymbol{P_{4s}}$ and then converted to vertical TEC by means of the single layer mapping function. MATLAB software called EGY_ION was developed to model (EIM). The performance of the developed Egyptian ionospheric map (EIM) WAS verified through the positioning accuracy of multi-constellation SFPPP for static and kinematic modes.

For static modes, local ionosphere model (EIM) had the highest accuracy amongst the other ionosphere models. Local ionosphere model (EIM) showed an improvements of (38%, 28%, and 42%) for accuracy of latitude, longitude, and altitude in comparison with Klobuchar

model, and (32%, 10%, and 37%) for accuracy of latitude, longitude, and altitude in comparison with GIM model, after session time of half an hour.

For kinematic mode, Local ionosphere model (EIM) showed improvements of (83%, 47%, and 62%) for accuracy of latitude, longitude, and altitude in comparison with Klobuchar model, and (57%, 65%, and 21%) for accuracy of latitude, longitude, and altitude in comparison with GIM model, after session time of half an hour.

REFERENCES

Abd Rabbou.M.& El-Rabbany. A. (2015), "*Multi-Constellation GNSS Single frequency PPP: An Efficient Technique for Low Cost Surveying Applications"*. Research poster, The Association of Ontario Land Surveyors, Huntsville, Canada. 26-28th February,2015.

Beran, T., (2008), *"Single-frequency, Single-receiver Terrestrial and Space-borne Point Positioning"*. PhD thesis, University of New Brunswick, Frederiction, New Brunswick, Canada

Bock, H., Jäggi, A., Dach, R., Schaer, S. and Beutler, G. (2009). *"GPS single-frequency orbit determination for low earth orbiting satellites"*. Advances in Space Research, 43(5), 783–791.

Chen, K. and Gao, Y. (2005). *"Real-time precise point positioning using single frequency data"*. Proceedings of ION GNSS 2005, 13–16 Sep 2005, Long Beach, California, USA, 1514–1523. Georgia, USA, 2400–2414.

Fei Guo, Xingxing Li, Xiaohong Zhang, Jinling Wang (2016), *"The contribution of Multi-GNSS Experiment (MGEX) to precise point positioning"*. Advances in Space Research 59 (2017) 2714–2725

Gao, Y., Zhang, Y. and Chen, K. (2006). *"Development of a real-time single-frequency precise point positioning system and test results"*. Proceedings of ION GNSS 2006, 26–29 Sep 2006, Fort Worth, Texas, USA, 2297–2303.

Hernández-Pajares et al. (2009), *"The IGS VTEC maps: a reliable source of ionospheric information since 1998"*. Journal of Geodesy, Volume 83, Issue 3-4, PP 263-275, March 2009. https://doi.org/10.1007/s00190-008-0266-1

Héroux, P., Y. Gao, J. Kouba, F. Lahaye, Y.Mireault, P. Collins, K. Macleod, P. Tétreault, and K. Chen (2004). "*Products and Applications for Precise Point Positioning - Moving Towards Real-Time*". *Proceedings of the 17th International Technical Meeting of the Satellite Division of the Institute of Navigation ION GNSS 2004, Long Beach, CA, September 21-24, 2004, 1832-1843.*

Hofmann-Wellenhof, B., Lichtenegger, H., and Wasle, E. (2008). *"GNSS - Global Navigation Satellite Systems"*. Springer-Verlag Wien.

Klobuchar, J. A. (1987). "*Ionospheric time-delay algorithm for single-frequency GPS users*". IEEE Transactions on Aerospace and Electronic Systems, 23(3), 325–331, doi: 10.1109/TAES.1987.310829.

Kouba J (2009) *"Testing of global pressure/temperature (GPT) model and global mapping function (GMF) in GPS analyses"*. Journal of Geodesy, 83(3–4):199–208

Krankowski A. and M. Hernandez-Pajares, (2016), "*LOFAR Ionospheric Workshop Space Research"*. Centre of the Polish Academy of Science, 2016.

Le, A. Q. and Tiberius, C. (2006). *"Single-frequency precise point positioning with optimal filtering".* GPS Solutions, 11(1), 61–69, doi: 10.1007/s10291-006-0033-9.

Leandro R., Langley R., Santos M.(2008). "*UNB3m_pack: A neutral atmosphere delay package for radiometric space techniques"*. GPS Solut. 2008;12:65–70.

Montenbruck O, Hauschild A, Steigenberger P (2014). "*Differential Code Bias Estimation Using Multi-GNSS Observations and Global Ionosphere Maps"*. Navigation 61(3) 191-201.

Montenbruck O, Steigenberger P, Khachikyan R, Weber G, Langley R.B, Mervart L, Hugentobler U, (2014). "*IGS-MGEX: Preparing the Ground for Multi-Constellation GNSS Science"*. 4th Int. Colloquium on Scientific and Fundamental Aspects of the Galileo System, Prague, 4-6 Dec 2013

Mostafa RABAH et al, (2018). *"Evaluation of the IGS-Global Ionospheric Mapping model over Egypt".* journal Annales Geophysicae., https://doi.org/10.5194/angeo-2018-92

Odijk, D., Teunissen, P. J. G. and Zhang, B. (2012). *"Single-frequency integer ambiguity resolution enabled precise point positioning".* Journal of Surveying Engineering, doi: 10.1061/(ASCE)SU.1943-5428.0000085.

Roma, David & Pajares, Manuel & Krankowski, Andrzej & Kotulak, Kacper & Ghoddousi-Fard, Reza & Yuan, Yunbin & Li, Zishen & Zhang, Hongping & Shi, Chuang & Wang, Cheng & Feltens, Joachim & Vergados, Panagiotis & Komjathy, Attila & Schaer, Stefan & García-Rigo, Alberto & Gómez Cama, José María. (2017) *"Consistency of seven different GNSS global ionospheric mapping techniques during one solar cycle"*. Journal of Geodesy. 10.1007/s00190-017-1088-9.

Schaer, S., Gurtner, W., Feltens, J.,(1998) *"IONEX: The Ionosphere Map Exchange Format Version 1",* Proceedings of the IGS AC Workshop, Darmstadt, Germany, 9.-11.

Schaer, S., G. Beutler, L. Mervart, M. Rothacher, and U. Wild (1995), *"Global and Regional Ionosphere Models Using the GPS Double Difference Phase Observable",* in IGS Workshop Proceedings on Special Topics and New Directions, edited by G. Gendt and G. Dick, pp. 77–92, GFZ, Potsdam, Germany, May 15–18, 1995.

Seeber, G., (2003), *"Satellite Geodesy"*. 2nd Edition, de Gruyter, Berlin, Germany

Simsky, A., (2006) *"Standalone Real-Time Navigation Algorithm for Single-Frequency Ionosphere-Free Positioning Based on Dynamic Ambiguities (DARTS-SF)".* Proceedings of ION GNSS 18th International Technical Meeting of the Satellite Division, Fort Worth, Texas, 301-308

Van Bree, R. J. P. and Tiberius, C. C. J. M. (2011). *"Real-time single-frequency precise point positioning: accuracy assessment".* GPS Solutions, doi: 10.1007/s10291-011-0228-6.

Wang et al (2016), *"Determination of differential code biases with multi-GNSS observations"*. Journal of Geodesy, Volume 90, Issue 3, pp.209-228. DOI: 10.1007/s00190-015-0867-4.

Øvstedal, O. (2002). "*Absolute positioning with single-frequency GPS receivers*". GPS Solutions, 5(4), 33–44, doi: 10.1007/PL00012910

Received: 2018-05-18,

Reviewed: 2018-11-05, 2018-11-09, and 2018-11-30,

Accepted: 2018-12-03.